Depth-Controlled β-NMR of ^{8}Li in a Thin Silver Film

G. D. Morris,[1] W. A. MacFarlane,[2,3] K. H. Chow,[4] Z. Salman,[3] D. J. Arseneau,[3] S. Daviel,[3] A. Hatakeyama,[3]
S. R. Kreitzman,[3] C. D. P. Levy,[3] R. Poutissou,[3] R. H. Heffner,[1] J. E. Elenewski,[5] L. H. Greene,[5] and R. F. Kiefl[3,6]

[1]*Los Alamos National Laboratory, K764, Los Alamos, New Mexico 87545, USA.*
[2]*Department of Chemistry, University of British Columbia, Vancouver V6T 1Z1, Canada.*
[3]*TRIUMF, 4004 Wesbrook Mall, Vancouver, British Columbia V6T 2A3, Canada.*
[4]*Department of Physics, University of Alberta, Edmonton, Alberta, Canada.*
[5]*Department of Physics, University of Illinois, Urbana Champaign, Illinois 61801, USA.*
[6]*Department of Physics, University of British Columbia, Vancouver, British Columbia V6T 1Z1, Canada.*

Depth-controlled β-NMR can be used to probe the magnetic properties of thin films and interfaces on a nanometer length scale. A 30 keV beam of highly spin-polarized ^{8}Li$^+$ ions was slowed down and implanted into a 50 nm film of Ag deposited on a SrTiO$_3$ substrate. A novel high field β-NMR spectrometer was used to observe two well resolved resonances which are attributed to Li occupying substitutional and octahedral interstitial sites in the Ag lattice. The temperature dependence of the Knight shifts and spin relaxation rates are consistent with the Korringa law for a simple metal, implying that the NMR of implanted ^{8}Li reflects the spin susceptibility of bulk metallic silver.

In the study of nanoscale materials, techniques such as electron and scanning probe microscopies and other surface sensitive methods have proven extremely useful. On the other hand, nuclear magnetic resonance (NMR), a very powerful technique in the study of *bulk* condensed matter, cannot generally be applied to nanoscopic systems as it requires a large number ($\sim 10^{20}$) of nuclei for a measurable signal. One powerful way to circumvent this limitation is to implant probes that are already highly spin polarized into the material of interest, such as low energy muons [1] or other types of radioactive ions. Along these lines, we have developed a novel instrument based on the β-NMR method [2] employing a highly spin-polarized radioactive ion beam. In β-NMR the nuclear resonance and relaxation of the probe are detected via the parity-violating weak β decay [3]. This nuclear method of detection is sensitive enough to detect the presence of a single probe nucleus, while a total of a few million implanted nuclei makes up a typical spectrum. In condensed matter studies, β-NMR has found many applications, including the study of isolated defects in semiconductors [4], and more recently, has even been used for surface science [5].

The novel features of our β-NMR instrument are the high magnetic field (9 T) and the ability to control the depth of implantation on the 2–200 nm range. Depth-controlled β-NMR represents a significant advance in magnetic resonance techniques. In the present study this depth control was used to obtain β-NMR signals in a thin silver film by reducing the implantation energy of ^{8}Li$^+$ to a low fixed value such that the ^{8}Li$^+$ stops entirely in the film [6]. The spectrum in high magnetic fields consists of two well resolved resonances that are attributed to Li at the octahedral and substitutional sites. The temperature

dependence of the Knight shifts and spin relaxation rates are consistent with a Korringa law.

Experiments were performed using the high field β-NMR spectrometer and radioactive ^{8}Li$^+$ beam at the ISAC radioactive beams facility at TRIUMF. ISAC delivers a continuous beam of $\sim$30 keV ^{8}Li$^+$ with a typical flux of 10^7/s in a beam spot 2–3 mm in diameter. Polarization of the ^{8}Li nuclear spin is achieved in a section of the beam line by in-flight optical pumping [7]. Here, the Li$^+$ beam is first neutralized by electron capture from a low density Na vapour. The neutral beam, still at 30 keV, drifts 2 m while the doppler-shifted $D1$ transition ($\lambda \sim 671$ nm) is pumped with a counter-propagating beam of circularly polarized laser light. At the end of the drift region the atomic beam is reionized in a He gas cell which strips one electron from the Li^0, allowing subsequent electrostatic steering and deceleration of the now spin-polarized beam. This design can routinely attain high polarizations (up to $\sim$70%) [8] while isolating the sample from the laser light.

Figure 1 shows the schematic of the spectrometer. The beam enters from the left, passing through an aperture in the backward β detector (B). It is then focused onto the sample by a combination of an electrostatic Einzel lens and the strong magnetic field H_0 of the superconducting solenoid (up to 9 T). The sample (typical area 8×10 mm) is mounted on a coldfinger cryostat situated in ultrahigh vacuum (UHV) ($\sim 10^{-9}$ Torr). A nonresonant "transmission line" Helmholtz coil straddles the sample and introduces a cw or pulsed rf magnetic field H_1 perpendicular to the static field H_0. The spin-2 ^{8}Li nucleus has a lifetime $\tau = 1.21$ s, a gyromagnetic ratio $^8\gamma = 630.15$ Hz/G, and an electric quadrupole moment $Q = +33$ mb. When the Li decays, a high energy β electron is
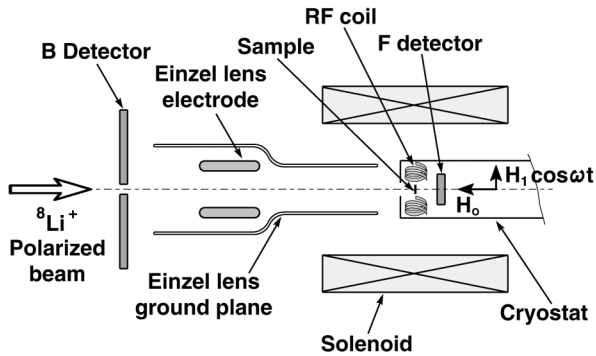
FIG. 1.   Schematic of the ISAC β-NMR spectrometer.

FIG. 2 (color online).   (a) The Ag β-NMR spectrum at 4 K in a field $H_0 = 0.3$ T and $H_1 \approx 3$ μT. The solid line is a fit to a Lorentzian line shape. The inset shows the linewidth (HWHM) of this resonance as a function of temperature. (b) At $H_0 = 3.0$ T and $T = 145$ K two signals are resolved. The vertical dashed line indicates the reference frequency in MgO. Typical spectra accumulated 35–100 $\times$ 10^6 decay events in 10–20 min. The inset shows the octahedral (O) and tetrahedral (T) interstitial sites and the substitutional site (S) in the fcc Ag lattice.

emitted preferentially in the direction opposite its spin. These βs are detected by fast plastic scintillation detectors (F and B). The Li spin polarization is proportional to the asymmetry ($\mathcal{A}$) in the counting rates: $\mathcal{A} = (F - B)/(F + B)$. Resonance spectra are obtained by slowly sweeping the frequency of the cw magnetic field H_1. When the frequency matches the splitting of the relevant Li energy levels, polarization is reduced as the Li magnetic moment precesses. Thus, the resonance signal appears as a loss of asymmetry. The spin-lattice relaxation rate $1/T_1$ can be measured by pulsing the incoming $^8Li^+$ beam with an electrostatic chopper and monitoring the time dependence of $\mathcal{A}$ after each pulse with no rf field. The depth of implantation is controlled by biasing the sample, cryostat, and solenoid which are all mounted on an isolated platform. This deceleration occurs between the Einzel lens ground plane and the sample.

The sample is a Ag film grown via thermal evaporation onto an ambient temperature single crystal $\langle 100 \rangle$ SrTiO$_3$ substrate (Applied Technology) at about 1 Å/s in a background pressure of $\sim 3 \times 10^{-7}$ Torr. A calibrated thickness rate monitor was used to estimate the film thickness at 500 Å.

In order to obtain a β-NMR signal from the silver film the beam was slowed down from 30 keV to 5 keV where the average depth of implantation occurs close to the center of the film. Figure 2(a) shows a typical resonance spectrum obtained at an applied magnetic field $H_0 = 0.3$ T. At all temperatures (T), there is a single narrow resonance very close to the Larmor frequency, indicating that the Li stops at sites of local cubic symmetry. Otherwise, quadrupolar coupling of the Li nucleus to the local electric field gradient would significantly modify the resonance. This indicates the Li is isolated from damage created by its implantation, behavior common for light ions implanted in solids. There are three candidate sites of cubic symmetry in the fcc lattice of silver; the octahedral (O) and tetrahedral (T) intersitial sites and the substitutional (S) site. The lack of structure in the line at low temperature [Fig. 2(a)], where the Li is not mobile, suggests that the narrowing shown in the inset is not due to motional averaging. On the other hand, it could be due to a compound line consisting of several unresolved
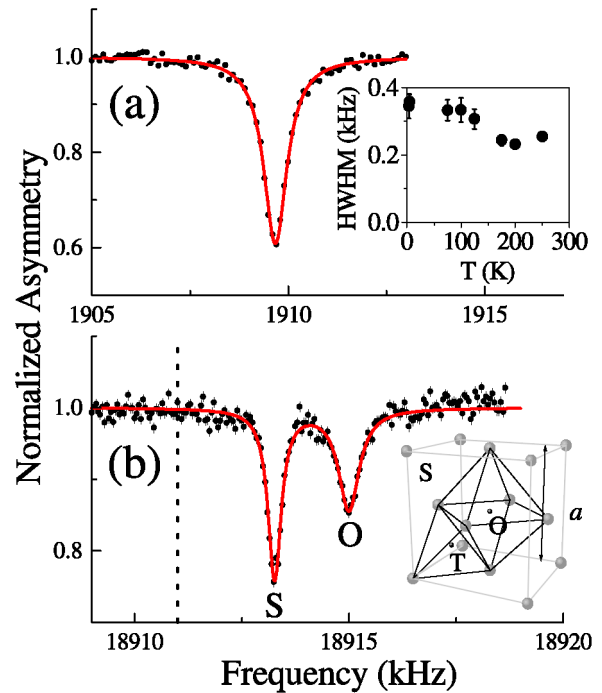
components whose amplitudes change with temperature. The spectrum at tenfold higher H_0 (3 T) shown in Fig. 2(b) confirms this latter possibility. At room temperature there is a single narrow resonance shifted by $+120(12)$ ppm with respect to the resonance observed in the cubic insulator MgO. As T is lowered, this signal decreases in amplitude while another resonance at $+212(15)$ ppm grows at its expense. The spectrum becomes T independent below about 100 K. This T dependence of the amplitudes and positions of the resonances is shown in Fig. 3 [9]. Preliminary experiments [10] on another less well characterized Ag film showed very similar behavior, confirming that this behavior is intrinsic to Ag. The shift we observe is a common effect in the NMR of metals, where it is due to coupling of the nuclei to the paramagnetic Pauli spin susceptibility of the conduction electrons, i.e., a Knight shift [11]. The very slight dependence on T may be related to thermal contraction effects as has been found in the NMR of Ag [12]. Notice the sum of the normalized amplitudes [Fig. 3(b)] exceeds one in the transition region, implying that each Li atom spends some fraction of its lifetime in both sites, and thus contributes to both resonances. This confirms that the observed T dependence of resonance amplitudes results
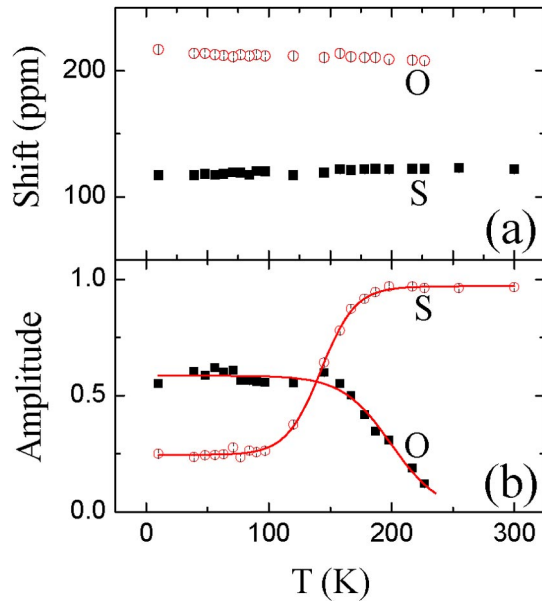
FIG. 3 (color online). Temperature dependences of (a) shifts with respect to ^{8}Li in MgO and (b) normalized amplitudes for $H_0 = 3.0$ T and $H_1 = 6$ μT. The solid lines are guides to the eye.

from a thermally induced transition between sites rather than T dependent occupation probabilities.

These results indicate that Li stops in two inequivalent cubic sites in the Ag lattice. At $T \leq 100$ K the Li is static, while at higher temperatures Li diffuses quickly to its most stable site, likely that of a vacancy created during the implantation process. We assign the low T (high frequency) line to Li trapped in a metastable O site. In this scenario, the high T (low frequency) line corresponds to the S site. These site assignments are consistent with other β-NMR [2] and channeling [13] experiments in similar systems. For example, for ^{12}B implanted in fcc copper, β-NMR cross-relaxation measurements clearly show that boron occupies the O site at low temperatures, but moves to the S site at high T [14]. It is not surprising that there is enough thermal energy to allow Li to make a site change. For example, interstitial Li, which has been studied in a variety of materials in connection with ionic conductivity and lightweight alloys [15], often becomes mobile in the range 200–300 K. The resonance *linewidths* also contain information about the Li site, as is illustrated by previous β-NMR studies of ^{12}B and ^{8}Li in Cu [16,17]. In particular, the resonance of the Li is broadened by the randomly oriented host lattice nuclear dipoles ($^{107,\ 109}$Ag). A simple estimate of this dipolar linewidth [18] predicts the O site resonance should be twice as broad as the S line, while we find experimentally [Fig. 2(b)] that it is about 1.5 times the width.

The measured Knight shift also provides site information as it is a fingerprint of the local electronic structure around the implanted Li. The Knight shift for a given site arises from the hybridization of the local (primarily, Li 2s) electron with the conduction band. This hybridization

determines the hyperfine coupling A, defined by $K = ZA(\chi_s/N_A)/g\mu_B$, where K is the Knight shift of Li; Z is the coordination of the Li site (12, 6, and 4 for S, O, and T respectively); $g\mu_B$ is the magnetic moment of the electron, and χ_s/N_A is the magnetic susceptibility per Ag atom. In our experiment, the two sites are thus primarily distinguished by their hyperfine couplings. Using $\chi_s = 9.6 \times 10^{-6}$ emu/mol [19], we obtain $A_S = 5.8$ and $A_O = 20.5$ kG/μ_B for the two sites, in qualitative agreement with the expectation that the more confined octahedral site is associated with the larger hyperfine coupling. Note that the hyperfine coupling of ^{7}Li in bcc Li metal (6.9 kG/μ_B [20]) is in the same range as our measurements. It is interesting to contrast these results with those for ^{12}B in Cu [16] where two resonances of ^{12}B are only partially resolved due to the much lower magnetic field. In contrast to ^{8}Li in Ag, the high temperature (S site) line is at *higher* frequency than the O site line. Detailed calculations of the electronic structures of the B and Li defects in Cu and Ag will be necessary to understand these differences [21].

Spin relaxation data obtained at several T, for $H_0 = 3$ T applied parallel to the initial Li spin, are shown in Fig. 4. Beam was admitted in 1 s pulses every 21 s, and typically 4×10^7 decay events were accumulated at each temperature. Generally the relaxation of nuclear spin polarization is caused by transverse magnetic fields fluctuating at the nuclear Larmor frequency [11]. In a metal, these dynamic fields are often dominated by contributions from random spin-flip scattering of the conduction electrons from the nuclei. The defining feature of this type of relaxation is its linear temperature dependence, usually expressed as the Korringa law,

$$\frac{1}{T_1 T K^2} = \frac{4\pi k_B}{\hbar}\left(\frac{^8\gamma}{\gamma_e}\right)^2 = 8.32 \times 10^4 \text{ K}^{-1}\text{s}^{-1}, \quad (1)$$

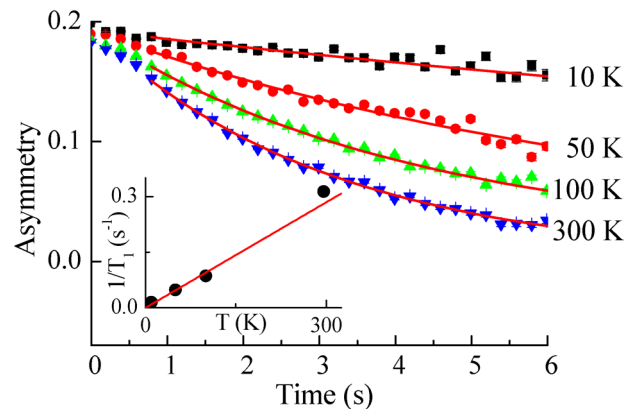where γ_e is the electron gyromagnetic ratio. In order to

FIG. 4 (color online). Longitudinal spin relaxation spectra recorded in $H_0 = 3.0$ T at several temperatures. Inset: Spin-lattice relaxation rate of the component assigned to the S site. The fit of the data to a straight line yields $1/T_1 = 0.00095$ s^{-1}K^{-1}T.

account for the site change discussed above, we fit the relaxation data to a sum of two exponential relaxations with the ratio of the relaxation rates fixed to the square of the ratio of the shifts. This simplification is based on the minimal assumption that the shift scales with the hyperfine coupling whereas the relaxation rate scales with A^2. It does not assume a particular mechanism for the relaxation, nor a particular temperature dependence to the quantities. In addition we used the relative amplitudes [Fig. 3(b)] to further constrain the fitting function. The extracted relaxation rate (for the S site) is plotted as a function of T in the inset of Fig. 4. The linear dependence provides strong confirmation of our model that implanted Li NMR reflects its coupling to the Ag conduction band. From the slope of this line, the experimental value of the Korringa constant is $6.6 \pm 1.3 \times 10^4$ $K^{-1}s^{-1}$ which compares well with the theoretical value above [11]. Note that the measured T_1 at room temperature is consistent with another measurement in a very different experimental situation [22], further confirming the behavior to be intrinsic. The validity of the Korringa law indicates that ^{8}Li senses a local electronic susceptibility in the thin metal film that is close to that of bulk silver.

There are many possible applications of this result in the study of thin films, interfaces and near surface phenomena, where conventional NMR is difficult or impossible. For example, one expects finite size effects to become important in studies of thin metallic or superconducting films and multilayers as the dimensions are reduced further. Additionally, one can evaporate noble metals like Ag onto the surface of nearly any material and use depth-controlled β-NMR to monitor the local static and dynamic magnetic fields near the interface. This could be applied, for instance, to search for weak surface magnetism in materials such as cuprate superconductors [23]. We estimate the sensitivity to changes in the local internal magnetic field to be about 0.1 G. A similar capability has been demonstrated recently for low energy muons [1]. However, the muon and ^{8}Li are very different and complementary probes of matter. In particular ^{8}Li lives about a million times longer. Consequently it is sensitive to processes that occur on a much longer time scale, such as Korringa relaxation, which is generally not observable with the short lived muon. Furthermore, the intrinsic frequency resolution of β-NMR is much greater as demonstrated here by the fact that Knight shifts as small as 100 ppm are easily resolved.

In summary, we have performed depth-controlled β-detected NMR of ^{8}Li in a 50 nm film of silver. In a high magnetic field of 3 T, two resonances are clearly resolved and are attributed to Li at the octahedral interstitial and substitutional sites. Above 100 K there is a thermally activated transition from the octahedral to substitutional sites such that at room temperature only the substitutional site is observed. The temperature dependence of the Knight shifts and spin-lattice relaxation

rates are consistent with the Korringa law. This work demonstrates a novel way to apply a form of nuclear magnetic resonance to studies of the magnetic properties of thin films, interfaces, and near surface phenomena.

[1] e.g., Ch. Niedermayer et al., Phys. Rev. Lett. **83**, 3932 (1999).

[2] H. Ackermann, P. Heitjans, and H.-J. Stöckmann in *Hyperfine Interactions of Radioactive Nuclei* edited by J. Christiansen, Topics in Current Physics Vol. 31 (Springer, Berlin, 1983), p. 291.

[3] e.g., E. Ségré, *Nuclei and Particles* (Benjamin, NY, 1965).

[4] e.g., F. Kroll et al. Physica B (Amsterdam) **308-310**, 989 (2001).

[5] e.g., H. Winnefeld et al., Phys. Rev. B **65**, 195319 (2002).

[6] T. R. Beals et al. Physica B (Amsterdam) **326**, 205 (2003).

[7] *Optical Orientation*, edited by F. Meier and B. P. Zakharchenya (Elsevier, Amsterdam, 1984).

[8] A. Hatakeyama et al., *Proceedings of the Ninth International Workshop on Polarized Sources and Targets*, edited by V. P. Derenchuk and B. von Przewoski (World Scientific, Singapore, 2002) p. 339.

[9] The resonances at 3 T are obtained at higher rf field (6 μT) than in Fig. 2(b) and hence have a larger amplitude and are slightly power-broadened.

[10] W. A. MacFarlane et al. Physica B (Amsterdam) **326**, 213 (2003).

[11] e.g., C. P. Slichter *Principles of Magnetic Resonance* (Springer, NY, 1990).

[12] U. El-Hanany, M. Shaham, and D. Zamir, Phys. Rev. B **10**, 2343 (1974).

[13] H. Hoffsass and G. Lindner, Phys. Rep. **201**, 121 (1991).

[14] M. Füllgrabe et al., Phys. Rev. B **64**, 224302 (2001), and references therein.

[15] T. Kudo and K. Fueki *Solid State Ionics* (VCH, NY, 1990); *Fourth International Aluminum-Lithium Conference*, edited by G. Champier, [J. Phys. Coll. 48, No. C3 (1987)].

[16] R. E. McDonald and T. K. McNab, Phys. Lett. A **63**, 177 (1977); Phys. Rev. B **13**, 34 (1976).

[17] F. Ohsumi et al. Hyperfine Interact. **120-121**, 419 (1999).

[18] J. H. van Vleck, Phys. Rev. **74**, 1168 (1948).

[19] G. C. Carter, L. H. Bennett, and D. J. Kahan, *Metallic Shifts in NMR* (Pergamon, Oxford, 1977).

[20] H. Brom and J. J. van der Klink, Prog. Nucl. Magn. Reson. Spectrosc. **36**, 89 (2000), and references therein.

[21] Preliminary calculations by M. Ogura, unpublished.

[22] I. Koenig et al., Z. Phys. A: At. Nucl. **A318**, 135 (1984).

[23] M. Covington et al., Phys. Rev. Lett. **79**, 277 (1997); R. Carmi et al. Nature (London) **404**, 853 (2000).